



# Lawrence Berkeley Laboratory

UNIVERSITY OF CALIFORNIA

## CHEMICAL BIODYNAMICS DIVISION

Submitted to Cancer Research

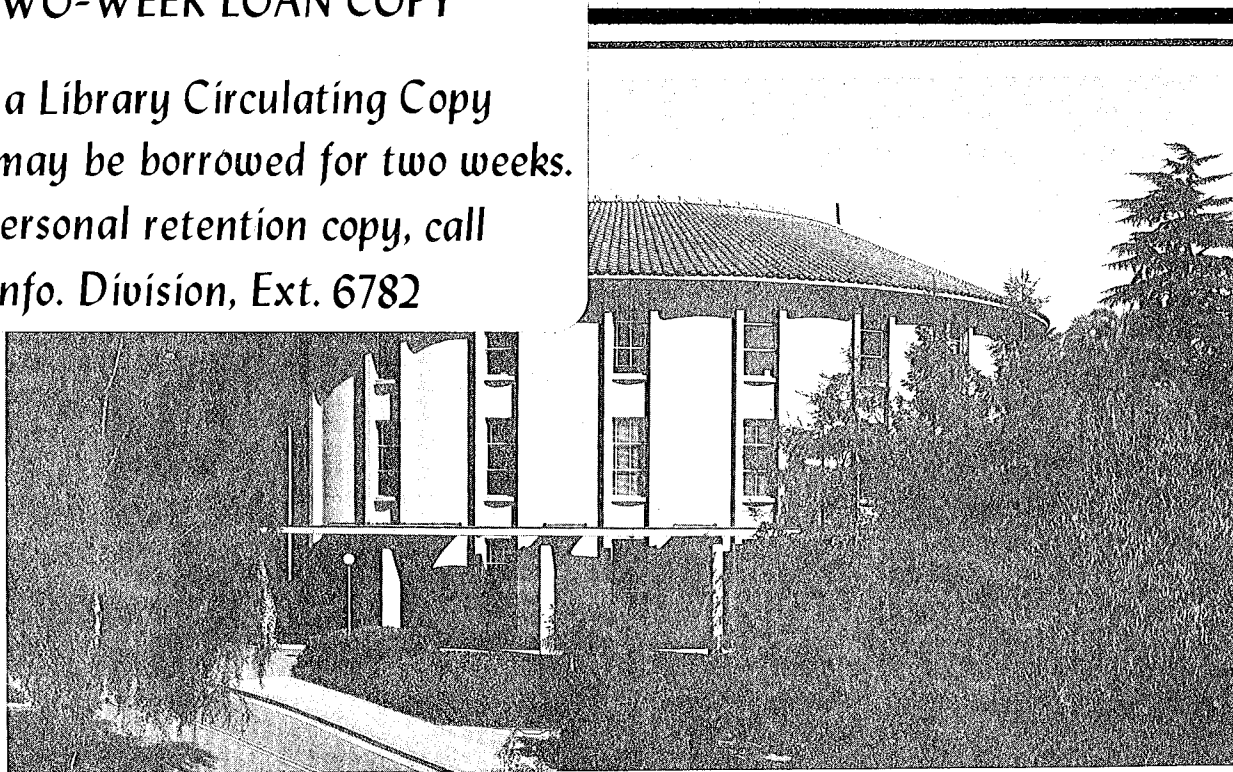
BENZO[a]PYRENE DIOL EPOXIDE PERTURBATION OF CELL CYCLE  
KINETICS OF SYNCHRONIZED MOUSE LIVER EPITHELIAL CELLS

Andrew L. Pearlman, Bruce N. Navsky, and James C. Bartholomew

July 1980

### TWO-WEEK LOAN COPY

*This is a Library Circulating Copy  
which may be borrowed for two weeks.  
For a personal retention copy, call  
Tech. Info. Division, Ext. 6782*



*LBL-11226  
c.2*

BENZO[a]PYRENE DIOL EPOXIDE PERTURBATION OF CELL CYCLE KINETICS  
OF SYNCHRONIZED MOUSE LIVER EPITHELIAL CELLS

Laboratory of Chemical Biodynamics  
Lawrence Berkeley Laboratory  
University of California  
Berkeley, California 94720  
USA

Andrew L. Pearlman  
Technicon Instruments Corporation  
511 Benedict Ave.  
Tarrytown, New York 10591  
USA

Bruce N. Navsky  
International Business Machines Corporation  
1322 Space Park Dr.  
Houston, Texas 77058  
USA

James C. Bartholomew  
Laboratory of Chemical Biodynamics  
Lawrence Berkeley Laboratory  
University of California  
Berkeley, California 94720  
USA

Address Correspondence To: Dr. James C. Bartholomew  
Laboratory of Chemical Biodynamics  
Lawrence Berkeley Laboratory  
University of California  
Berkeley, California 94720

(415) 486-4300

Running Title: BaP Diol Epoxide Perturbation of NMuLi  
Cell Cycle

### SUMMARY

A cell cycle synchronization system is described for the analysis of the perturbation of cell cycle kinetics and the cycle-phase specificity of chemicals and other agents. We used the system to study the effects of ( $\pm$ )r-7, t-8-dihydroxy-t-9, 10-oxy-7,8,9,10-tetrahydrobenzo[a]pyrene (BaP diol epoxide) upon the cell cycle of mouse liver epithelial cells(NMuLi).

BaP diol epoxide(0.6  $\mu$ M) was added to replated cultures of NMuLi cells that had been synchronized in various stages of the cell cycle by centrifugal elutriation. DNA histograms were obtained by flow cytometry as a function of time after replating. The data were analyzed by a computer modeling routine and reduced to a few graphs illustrating the "net effects" of the BaP diol epoxide relative to controls. BaP diol epoxide slowed S-phase traversal in all samples relative to their respective control. Traversal through  $G_2M$  was also slowed by at least 50%. BaP diol epoxide had no apparent effect upon  $G_1$  traversal by cycling cells, but delayed the recruitment of quiescent  $G_0$  cells by about 2 hrs.

The methods described constitute a powerful new approach for probing the cell cycle effects of a wide variety of agents. The present system appears to be extremely sensitive and capable of characterizing the action of agents on each phase of the cell cycle. The methods are automatable and would allow for the assay and possible differential characterization of mutagens and carcinogens.

## INTRODUCTION

Many authors(11, 12, 13) argue that chemical substance account for a large proportion of the environmental carcinogens, and that many of these chemicals are industrial in origin. In particular, effluents released as biproducts of incomplete combustion of fossil fuels include a wide variety of PAH's<sup>1</sup> which have been shown to be both mutagenic and carcinogenic(11). The expected increase in the use of fossil fuels as energy sources has raised concern regarding the potential increase in carcinogenic and mutagenic risk that will be generated. This concern has spurred the development of several putative assays for carcinogens and mutagens(1, 19).

Like many other PAH's, BaP has been shown to require enzymatic conversion to an active form which is then capable of interaction with cellular macromolecules(2, 7, 21, 22, 27). The metabolic activation of BaP has been the subject of intensive investigation during the past several years from which has emerged the consensus that the ultimate carcinogenic derivative of BaP produced by the aryl hydrocarbon hydroxylase metabolism is the BaP diol epoxide(21, 26).

BaP diol epoxide has been shown to form adducts with

<sup>1</sup> The abbreviations used are: PAH, polycyclic aromatic hydrocarbons; BaP, benzo[a]pyrene; BaP diol epoxide, (±)7, 8-dihydroxy-7,8,9,10-tetrahydrobenzo[a]pyrene; saline GM, 1.5mM Na<sub>2</sub>HPO<sub>4</sub>, 1.1 mM KH<sub>2</sub>PO<sub>4</sub>, 1.1 mM glucose, and 0.14 M NaCl, at pH 7.4; DMSO, dimethylsulfoxide.

DNA bases(5, 16, 18, 24, 25), and there is evidence that such adduct formation slows or halts DNA replication(3, 8, 19). Cell culture experiments have demonstrated that treatment during the S-phase of the cell cycle with carcinogens results in the highest transformation frequency(4, 15, 17). These findings and other suggest that direct interference in normal DNA synthesis may be a primary mechanism in malignant transformation of cells.

In probing this hypothesis, Bartholomew et al.(3) investigated the cell cycle effects of various metabolites of BaP, including BaP diol epoxide, in asynchronously growing, and in serum stimulated cultures of mouse liver epithelial cells. Of all the metabolites tested, BaP diol epoxide produced the most dramatic cell cycle perturbations which involved a general increase in the fraction in S-phase.

In this study, we have employed several new methods to determine the effects of BaP diol epoxide upon subpopulations of cells enriched in different cell cycle phases. Our overall approach (Chart 1) was to fractionate a large growing population of cells into samples enriched in the various stages of the cell cycle by elutriation centrifugation. Each sample was then split into control and treated batches, and replated in multiple cultures for sampling at subsequent time intervals. Parallel sets of DNA histograms of the BaP diol epoxide treated and control populations were recorded

by flow cytometry at various time intervals. Then, from the time series of histograms we extracted a few "net effects" curves which depicted the time course of the differences between treated and control populations. These "net effects" curves were used to discern and compare trends in the kinetic behavior of the two parallel populations.

## MATERIALS AND METHODS

### 1. Cell Culture Technique

Monolayer cultures of the established epithelial cell line NMuLi, derived from the livers of Namru mice by Owens et al.(23), were seeded in 100 mm culture dishes(Falcon Plastics, Oxnard, Calif.) in Eagle's Minimal Medium(GIBCO, Grand Island, N. Y.), denoted here as MEM, with 10% donor calf serum (Flow Laboratories, Rockville, MD), and allowed to reach saturation density( $1.3 \times 10^5$  cells per  $\text{cm}^2$ ). At 60 hrs prior to elutriation, the cells were transferred at a 1 to 10 dilution into roller bottles (Falcon Plastics, Oxnard, Calif.). Transfer of cells from the dishes was done by washing the monolayers once with saline GM( $1.5 \text{ mM Na}_2\text{HPO}_4$ ,  $1.1 \text{ mM KH}_2\text{PO}_4$ ,  $1.1 \text{ mM glucose}$ , and  $0.14 \text{ M NaCl}$ , at pH 7.4) followed by trypsinization for 3 min at  $37^\circ \text{C}$  with saline GM containing  $0.5 \text{ mM EDTA}$  and  $0.1 \text{ mg/ml crystalline trypsin}$ (GIBCO, Grand Island, N. Y.). Trypsinized cells were removed from the surface of the dishes into saline GM containing  $6.3 \text{ mM MgSO}_4$ ,  $1.1 \text{ mM CaCl}_2$ ,  $0.2 \text{ mg/ml soybean trypsin inhibitor}$ (GIBCO),  $0.01 \text{ mg/ml DNase}$ (Worthington, Freehold, N. J.), and  $0.1\%$  bovine serum albumin(Sigma, St. Louis, Mo.).

For elutriation, medium was aspirated from 8 roller bottles and the cells were washed once with saline GM and trypsinized as described above to yield  $6.0 \times 10^8$  cells in 40 ml of suspension medium for loading into the elutriator.

Prior to loading the cells, the elutriation system was flushed with 70% ethanol, followed by rinsing with sterile suspension medium.

## 2. Elutriation

The cells were separated using a Beckman JE-6 elutriator rotor and associated J-21 centrifuge. Cell suspension medium was continuously driven through the system by peristaltic pump (Cole Parmer Masterflex, with 7014 head), and the sample was loaded through a post-pump valve at 10 ml/min via a syringe drive (Orion Instruments, Cambridge, Mass.). Fluid from the pump passed through a bubble trap prior to traversing a triflat flow meter (5-60 ml/min range, Manostat, New York, N. Y.), from which it passed directly into the elutriator rotor. The bubble trap also served to damp out the peristaltic pressure variations.

Upon exit from the rotor, fluid passed through a Beckman DB spectrophotometer equipped with a custom-built 4 cm pathlength flow cell capable of sustaining flow rates in excess of 500 ml/min (for flushing purposes). At an illumination wavelength of 600 nm, the optical detection system easily sensed cells emerging from the rotor in concentrations of  $2.0 \times 10^3$  cells/ml or greater.

Cells were routinely loaded with rotor speed set sufficiently high (typically 3500-4000 revolutions per minute for a counterflow rate of 25 ml/min) to minimize the washing out



of whole cells. Speed decrements began from this initial loading condition, and the spectrophotometer was adjusted to 100% transmittance under these conditions. The set of speed decrements for obtaining the desired cycle phase enrichments in the fractions was determined by a modeling routine, described below, calculated during the experiment by means of a programmable calculator.

### 3. DNA Histograms

Cell cycle distributions of all cell populations, both before and after elutriation, were obtained by staining the cells using the propidium iodide technique described by Crissman and Steinkamp (9) and analyzed in a flow cytometer constructed as described by Holm and Cram(14). A Spectra Physics Model 171 argon ion laser provided a 2.0 watt excitation beam at 488 nm wavelength. Individual histograms were normalized to constant total cell count, and gain-shifted to place the  $G_1$  peak mode in channel 100, to facilitate visual comparison. Quantitative data was obtained by analyzing the histograms with a deconvolution modeling program<sup>2</sup> to yield estimated population percent in  $G_1$ , S, and  $G_2M$ . These data sets extracted from each DNA histograms were stored for later comparison between treated and control histograms. Calculated difference spectra between treated and control data sets were generated for each time point as

<sup>2</sup>Pearlman, A. L., Navsky, B. N., and Bartholomew, J. C., Manuscript in preparation.

illustrated in Chart 2.

4. Carcinogen Addition

BaP diol epoxide was provided by Dr. Kenneth Straub. The BaP diol epoxide was dissolved in DMSO (1.0 mg/ml) prior to addition to the cells. Addition was made to the freshly elutriated cells just prior to replating in 100 mm dishes. The final BaP diol epoxide concentration was  $6 \times 10^{-7}M$  and the DMSO concentration was 0.2% in both control and carcinogen treated cultures.

## RESULTS

### 1. Inhibition of G<sub>1</sub> Traversal

A logarithmically growing population of cells was elutriated into fractions having the DNA content distributions shown in Chart 3. These elutriated fractions were then replated and treated with BaP diol epoxide as described in the MATERIALS AND METHODS section. Chart 4 presents the DNA histograms of cells from the F1 elutriated fraction after reseeding in the presence of BaP diol epoxide dissolved in DMSO, DMSO alone, or with no addition. F1 is the fraction most enriched in cells having G<sub>1</sub> DNA content. These cells do not move through the cell cycle monotonically, but appear to be composed of two kinetic species. The first cohort of cells moves through the cycle as G<sub>1</sub> cells; whereas, the second cohort moves into S with a lag characteristic of G<sub>0</sub> cells(6). DMSO is seen to have caused only minor perturbations in comparison to those of BaP diol epoxide, and was very similar to the untreated populations. The DNA histograms reveal that BaP diol epoxide did not inhibit G<sub>1</sub> traversal as judged by the transit time of the first cohort into early S-phase and on into G<sub>2</sub>M. As seen in Chart 4, this cohort of cells left G<sub>1</sub> at 4 hrs post replating in both control and BaP diol epoxide treated cultures. A second cohort of cells presumably arising from G<sub>0</sub> began entering S at about 8 hrs in the control; whereas, the second cohort did not reach S in the BaP diol epoxide treated cultures

until 10 hrs. This delayed arrival time indicates a 25% increase in the lag from  $G_0$  to S.

## 2. Inhibition of $G_2M$ Traversal

Progress through  $G_2M$  also appears to have been slowed by BaP diol epoxide, as seen in the histograms for sample F4 in Chart 5. A substantial proportion of the  $G_2M$  cells initially present, have divided by 6 hrs in the control populations resulting in a dramatic increase in the  $G_1$  fraction by this time. In the BaP diol epoxide treated cultures the  $G_1$  increase is not seen until 8 hrs indicating a 2 hr retardation of  $G_2M$  traversal. Some of this delay in the build-up  $G_1$  was caused by an inhibition of the S-phase cells in this fraction (see next section).

## 3. Susceptibility of S-Phase Cells to BaP Diol Epoxide

Fractions F2, F3, and F4 all had significant levels of S-phase cells. The movement of these cells through S and into  $G_2$  and the effect of BaP diol epoxide was difficult to visualize and quantify. In an attempt to overcome these difficulties we developed the technique described in the MATERIALS AND METHODS section for taking the difference of two DNA histograms. This technique is demonstrated in Chart 6 for fractions F1 and F3. These "net effects" curves compare experimental DNA histograms with control histograms by subtracting the proportion of cells in each cell cycle phase of the control from the corresponding proportion in the

experimental. Chart 6 demonstrates that the fraction containing the most S-phase cells (F3) is dramatically affected by the BaP diol epoxide. The cells are moving through S so slowly that the  $G_1$  cells move into S causing a net accumulation in that cell cycle phase. The proportion of cells in the  $G_2M$  phases begins to increase relative to control as this slow moving wave begins to leave S. This same data analysis technique applied to F2 and F4 also showed that the S-phase cells were most sensitive to the inhibitory effects of BaP diol epoxide.  $G_2M$  was the next most sensitive cell cycle phase followed by  $G_0$ . The  $G_1$  section of the cell cycle was hardly affected by the compound.

As seen in Charts 5 and 6, the BaP diol epoxide effects were not transient, but resulted in significantly different distribution in the cell cycle compared to controls as late as 28 hrs after treatment.

## DISCUSSION

The hypothesis that chemical carcinogens act by perturbing normal DNA synthesis cannot account for all the effects of BaP diol epoxide observed in this study. Progress through S-phase is indeed perturbed by BaP diol epoxide in all samples and the S-phase was shown to be more sensitive to BaP diol epoxide than other phases of the cell cycle. The study reported here demonstrates effects on cell cycle phases other than S. These observations imply that besides DNA synthesis, other important cellular function may be affected by BaP diol epoxide and thus be involved in its perturbation of the cell cycle.

The effects of BaP diol epoxide upon these cells are more complex than is the case with cell cycle perturbing agents such as hydroxyurea or thymidine. The BaP diol epoxide action can not be modeled by a single induced delay or block, rather a complicated combination of effects is indicated. Hydrolyzed BaP diol epoxide (Tetraol) is apparently not responsible for the observed effects since experiments analogous to these using asynchronous NMuLi cells have shown that the tetraol does not perturb the cell cycle(3). The long-lasting nature of the effects suggests incomplete repair of modifications caused by the BaP diol epoxide.

The use of differences between fitted experimental and control DNA histograms has enabled direct comparison of the response of cell populations with vastly different cell

cycle distributions at the time of agent addition. This "net effect" approach holds promise as a quantitative measure of cell cycle phase specificity of agent action though it stops short of a formal mathematical modeling of the cell cycle kinetics such as the approach of Gray (10).

Beyond this use, the present system may have potential for much broader use in assaying cell cycle effects of a wide variety of agents, including mutagens and carcinogens. Recent authors have explored the potential of testing the inhibition of DNA synthesis in mammalian cell cultures as an assay for mutagenesis in humans, and have shown good correlation to findings with the Ames bacterial mutagenesis assay(19). These methods, however, rely on the uptake of radioactively labeled thymidine and subsequent counting to detect inhibition of DNA synthesis. Hence, the sensitivity of the assay is limited by the effect of the test agent on the cellular uptake of thymidine and its actual incorporation into the cellular genome. The precision, reproducibility, and large sample size afforded by the use of high speed flow cytometry, as well as the availability of fluorescent dyes which bind specifically and stoichiometrically to DNA, make possible a greater sensitivity with the approach reported here. Also, this system is faster and far more easily automated than autoradiography, an important consideration for its practical use.

ACKNOWLEDGEMENTS

We gratefully acknowledge the valuable input of Hisao Yokota of our laboratory who helped us spot several important aspects of the data cited above. We also acknowledge the much needed assistance rendered us by Jean Lawson and Maria Decosta who made the cell culture aspects of this work possible. We also thank Sheldon Wong for implementing the simulated gain-shifting and area normalization programs on our computer, as well as the crucial data handling and storage software for the flow cytometer. We would also like to thank Dr. Leonard Orenstein for his valuable comments and critical reading of this manuscript.

This research was supported by the Division of Biomedical and Environmental Research, United States Department of Energy, under contract Number W-7405-ENG-48.



REFERENCES

1. Ames, B. N., McCann, J., and Yamasaki, E. Methods for detecting carcinogens and mutagens with the Salmonella/mammalian-microsome mutagenicity test. *Mutation Res.*, 31: 347-364, 1975.
2. Autrup, H., Wefald, F. C., Jeffrey, A. M., Tate, H., Schwartz, R. D., Trump, B. F., and Harris, C. C. Metabolism of benzo[a]pyrene by cultured tracheobronchial tissues from mice, rats, hamsters, bovines, and humans. *Int. J. Cancer*, 25: 293-300, 1980.
3. Bartholomew, J. C., Pearlman, A. L., Landolph, J. R., and Straub, K. Modulation of the cell cycle of cultured mouse liver cells by benzo[a]pyrene and its derivatives. *Cancer Res.*, 39: 2538-2543, 1979.
4. Bertram, J. S. Effects of serum concentration on the expression of carcinogen-induced transformation in the C3H/10T 1/2 cl 8 cell line. *Cancer Res.*, 37: 514-523, 1977.
5. Brookes, P., King, H. W. S., and Osborn, M. R. The interaction of polycyclic hydrocarbons with DNA and mammalian cells in culture. *In*: H. V. Gelboin and P. O. P. Ts'o (eds), POLYCYCLIC HYDROCARBONS AND CANCER, Vol. 2, PP. 43-50, Academic Press, New York (1978).
6. Brookes, R. F., Bennett, D. C., and Smith, J. A. Mammalian cell cycles need two random transitions. *Cell*, 19: 493-504, 1980.
7. Burke, M. D., Vadi, H., Jernstrom, B., and Orrenius, S. Metabolism of benzo[a]pyrene with isolated hepatocytes and the formation and degradation of DNA-binding derivatives. *J. Biol. Chem.*, 252: 6424-6431, 1977.
8. Chang, G. T., Harvey, r. G., Hsu, W. -T., and Weiss, S. B. Inactivation of SV40 replication by derivatives of benzo[a]pyrene. *Biochem. Biophys. Res. Commun.*, 88: 688-695, 1979.
9. Crissman, H. A., and Steinkamp, J. A. Rapid simultaneous measurement of DNA, protein and cell volume in single cells from large mammalian cell populations. *J. Cell Biol.*, 59: 766-771, 1973.
10. Gray, J. W. Cell cycle analysis of perturbed cell populations: Computer simulation of sequential DNA distributions. *Cell Tissue Kinetics*, 9: 499-516, 1976.

11. Heidelberger, C. Chemical carcinogenesis. *Ann. Rev. Biochem.*, 44: 79-121, 1975.
12. Higginson, J. In: ENVIRONMENT AND CANCER, 24th Symp. *Fundam. Canc. Res.* pp.69-92. Baltimore: Williams and Wilkins, 1972.
13. Higginson, J., and Muir, C. S. In: J. F. Holland, E. Frei III (eds.), *CANCER MEDICINE*, pp. 241-306. Philadelphia: Lea and Febiger, 1973.
14. Holm, D. M., and Cram, L. S. An improved flow micro-fluorometer for rapid measurement of cell fluorescence. *Expt. Cell Res.*, 80: 105-110, 1973.
15. Jones, P. A., Baker, M. S., Bertram, J. S., and Benedict, W. F. Cell cycle-specific oncogenic transformation of C3H/10T 1/2 clone 8 mouse embryo cells by 1-b-d-arabinofuranosylcytosine. *Cancer Res.*, 37: 2214-2217, 1977.
16. Koreeda, M., Moore, P. D., Wislocki, P. G., Levin, W., Conney, A. H., Yagi, H., and Jerina, D. M. Binding of benzo[a]pyrene 7,8-diol-9,10-epoxide to DNA, RNA, and protein of mouse skin occurs with stereoslectivity. *Science*, 199: 778-780, 1978.
17. Marquardt, H. Cell cycle dependence of chemically induced malignant transformation in Vitro. *Cancer Res.*, 34: 1612-1615, 1974.
18. Meehan, T., Straub, K., and Calvin, M. Benzo[a]pyrene diol epoxide covalently binds to deoxyguanosine and deoxyadensosine in DNA. *Nature*, 269: 725-727, 1977.
19. Painter, R. B., and Howard, R. A comparison of the HeLa DNA-synthesis inhibition test and the Ames test for screening of mutagenic compounds. *Mutation Res.*, 54: 113-115, 1978.
20. Petersen, A. R., Bertram, J. S., and Heidelberger, C. Cell cycle dependence of DNA damage and repair in transformable mouse fibroblasts treated with N-methyl-N'-nitro-N-nitrosoguanidine. *Cancer Res.*, 34: 1600-1607, 1974.
21. Pezzuto J. M., Yang, C. S., Yang, S. K., McCourt, D. W., and Gelboin, H. V. Metabolism of benzo[a]pyrene and (-)trans-7,8-dihydroxy-7,8- dihydrobenzo[a]pyrene by rat liver nuclei and microsomes. *Cancer Res.*, 38: 1241-1245, 1978.

22. Phillips, D. H., and Sims, P. In: Polycyclic aromatic hydrocarbon metabolites: Their reactions with nucleic acids. P. L. Grover (ed), CHEMICAL CARCINOGENS AND DNA, VOL.2, pp.29-58, CRC Press, Boca Raton, Fl. 1979.
23. Owens, R. B., Smith, H. S., Hackett, A. J. Epithelial cell cultures from normal glandular tissue of mice. J. Natl. Cancer Inst., 53: 261-269, 1974.
24. Remsen, J., Jerina, D. M., Yagi, H., and Cerutti, P. In Vitro reaction of radioactive 7<sup>a</sup>, 8<sup>a</sup>-dihydroxy-9<sup>a</sup>, 10<sup>a</sup>-epoxy-7,8,9,10-tetrahydrobenzo[a]pyrene with DNA. Biochem. Biophys. Res. Commun., 74: 934-940, 1977.
25. Weinstein, I. B., Jeffrey, A. M., Leffler, S., Pulkra-  
bek, P., Yamasaki, H., and Grunberger, D. Interaction  
between polycyclic aromatic hydrocarbons and cellular  
macromolecules. In: H. V. Gelboin and P. O. P. Ts'o  
(eds), POLYCYCLIC HYDROCARBONS AND CANCER, VOL 2., pp.  
1-36, New York: Academic Press, (1978).
26. Yang, S. K., McCourt, D. W., Roller, P. P., and Gel-  
boin, H. V. Enzymatic conversion of benzo[a]pyrene  
leading predominantly to the diol-epoxide r-7, t-8-  
dihydroxy-t-9,10-oxy-7,8,9,10- tetrahydrobenzo[a]pyrene  
through a single enantiomer of r-7, t-8-dihydroxy-7,8-  
dihydrobenzo[a]pyrene. Proc. Natl. Acad. Sci. USA, 73:  
2594-2598, 1976.
27. Yang, S. K., Deutsch, J., and Gelboin, H. V.  
Benzo[a]pyrene metabolism: Activation and detoxifica-  
tion. In: H. V. Gelboin and P. O. P. Ts'o (eds), POLY-  
CYCLIC HYDROCARBONS AND CANCER, VOL 1, pp. 205-231,  
Academic Press, New York (1973).

## CHART LEGENDS

### Chart 1. General experimental approach.

Cells in culture were harvested and fractionated into different phases of the cell cycle by centrifugal elutriation. Each enriched fraction was split into control and test batches, which were replated in fresh medium for sampling at subsequent time intervals. At each interval, DNA histograms of the various populations were recorded. The histograms were analyzed as described in Chart 2.

### Chart 2. Data reduction and analysis.

Corresponding test and control histograms for a given sample were fit using a deconvolution routine. Along with  $G_1$ , S, and  $G_2M$ , the routine divided S into 9 subcompartments so that a total of 12 values were estimated for each histogram. The control values were subtracted point-for-point from those of the test population to give the values used in the "net effects" curves.

### Chart 3. DNA histograms of the elutriated population used in these experiments.

The histogram labeled control is the original pre-elutriated population. Samples F1, F2, F3, and F4 were obtained at increasing relative sedimentation velocities. Fractions in each cycle phase listed next to the plots were determined from computer fits to the histograms.

### Chart 4. BaP diol epoxide effects of $G_1$ cells.

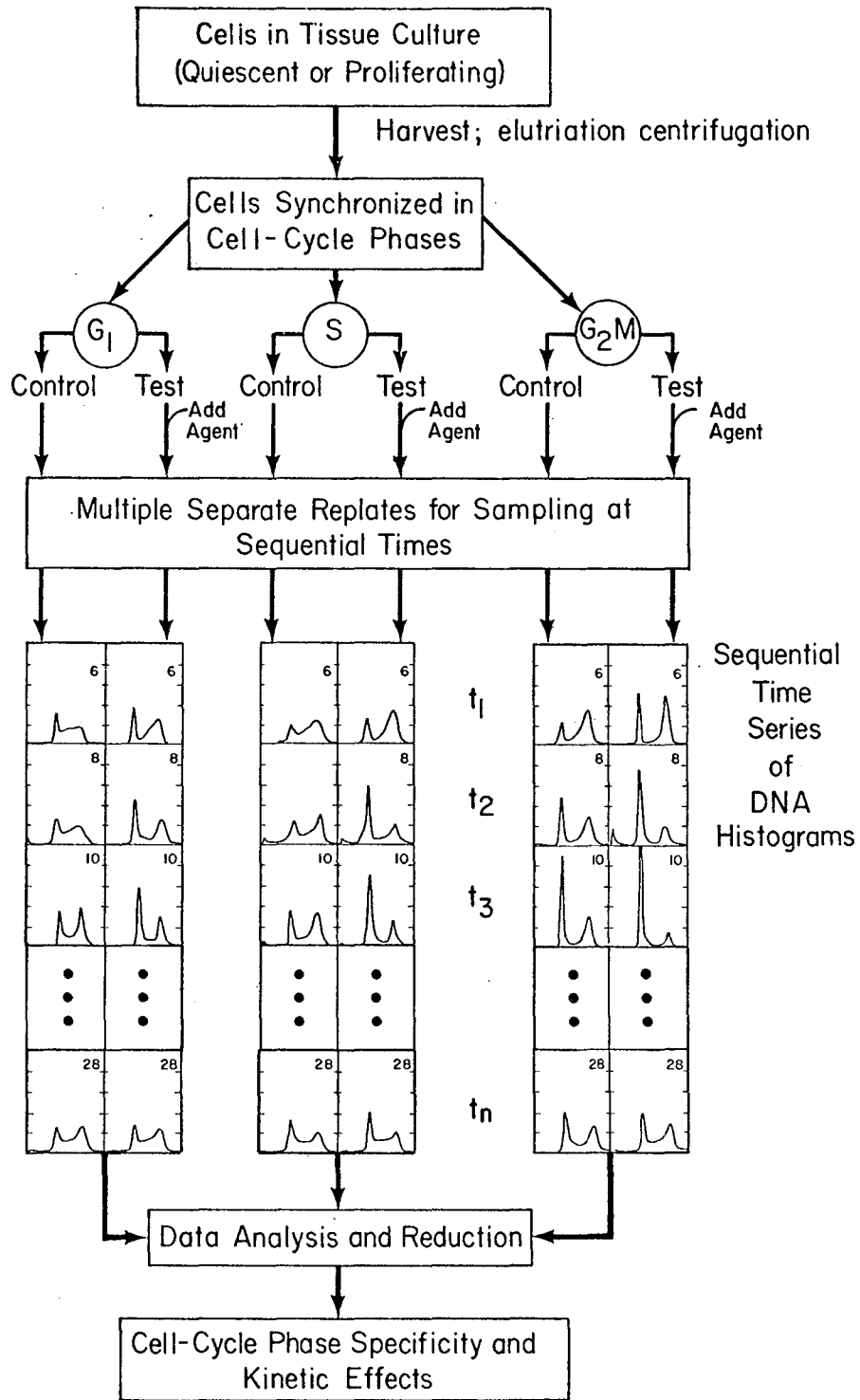
The numbers in the upper right-hand corner are the times after reseeded when the sample was harvested.

### Chart 5. BaP diol epoxide effects on S and $G_2$ .

The numbers in the upper right-hand corner are the times after reseeded when the sample was harvested.

### Chart 6. "Net effects" on samples enriched in $G_1$ (F1) or S-phase cells(F3).

Calculated differences between BaP diol epoxidized treated and control cycle phase percentages for samples F1 and F3.

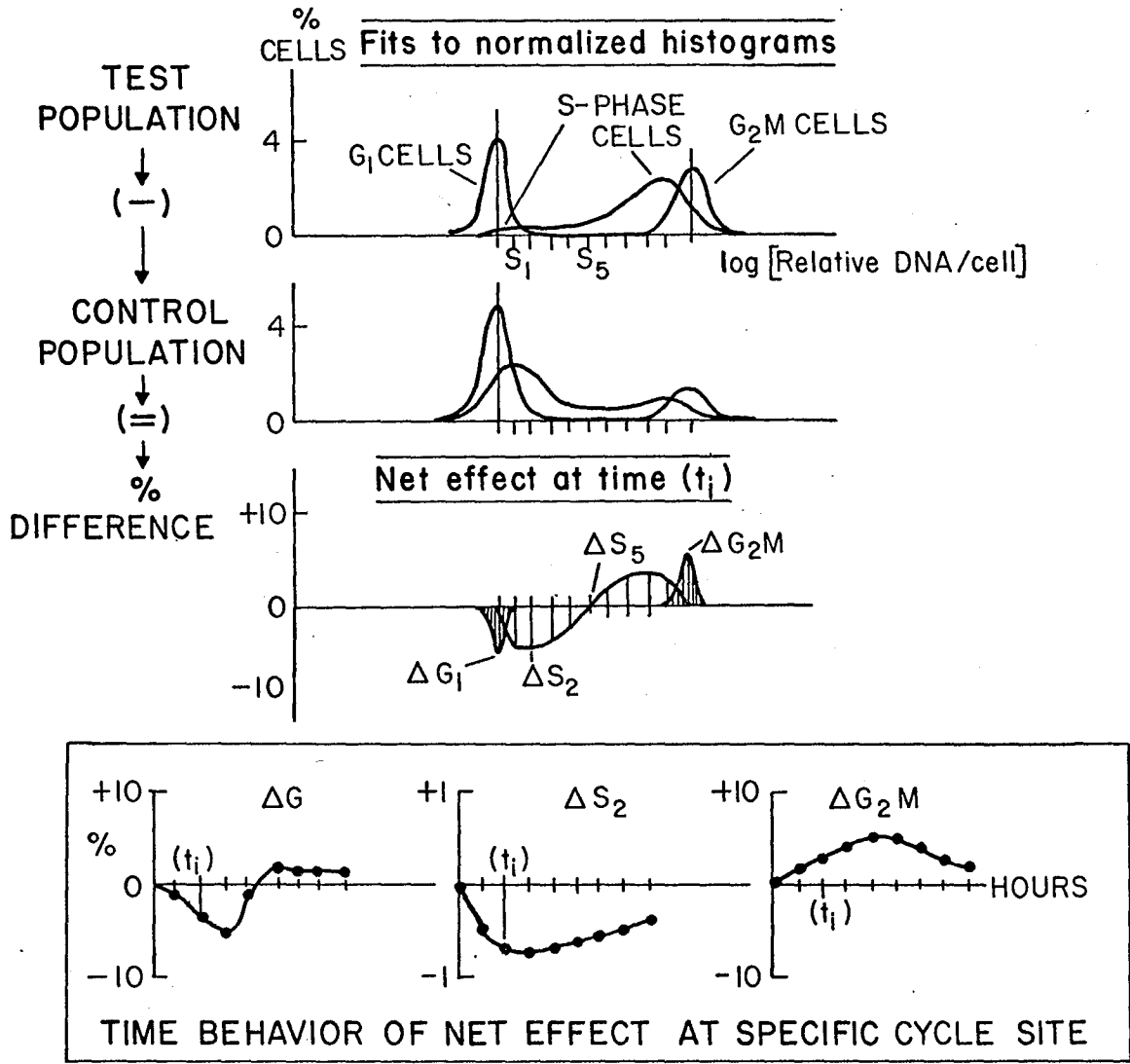


XBL 804-4159

Pearlman, Navsky, and  
Bartholomew

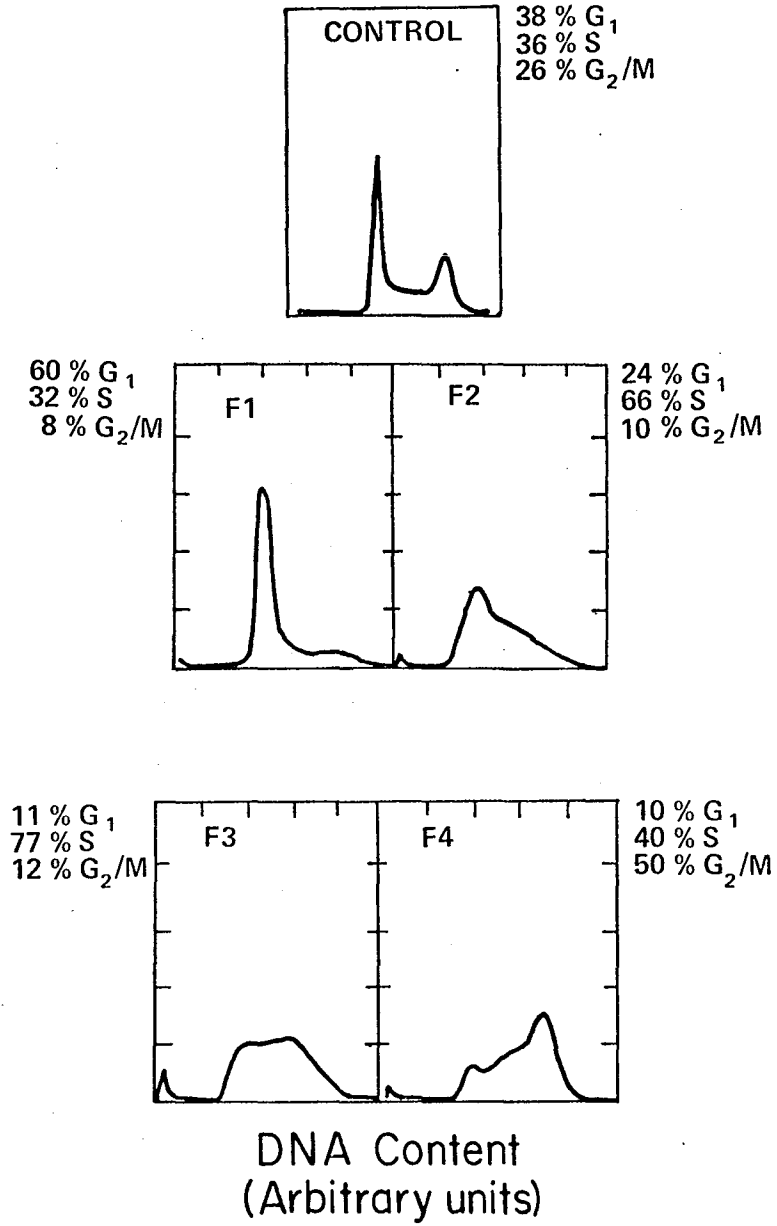
CHART 1

# DATA REDUCTION AND ANALYSIS



XBL 784 - 3931

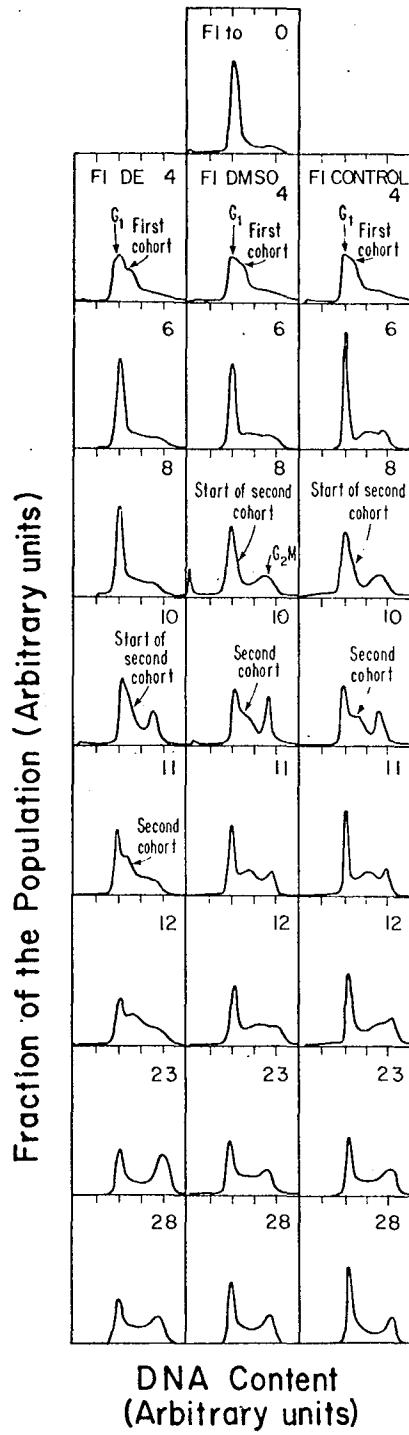
Fraction of the Population (Arbitrary units)



XBL 788-4174A

Pearlman, Navsky, and  
Bartholomew

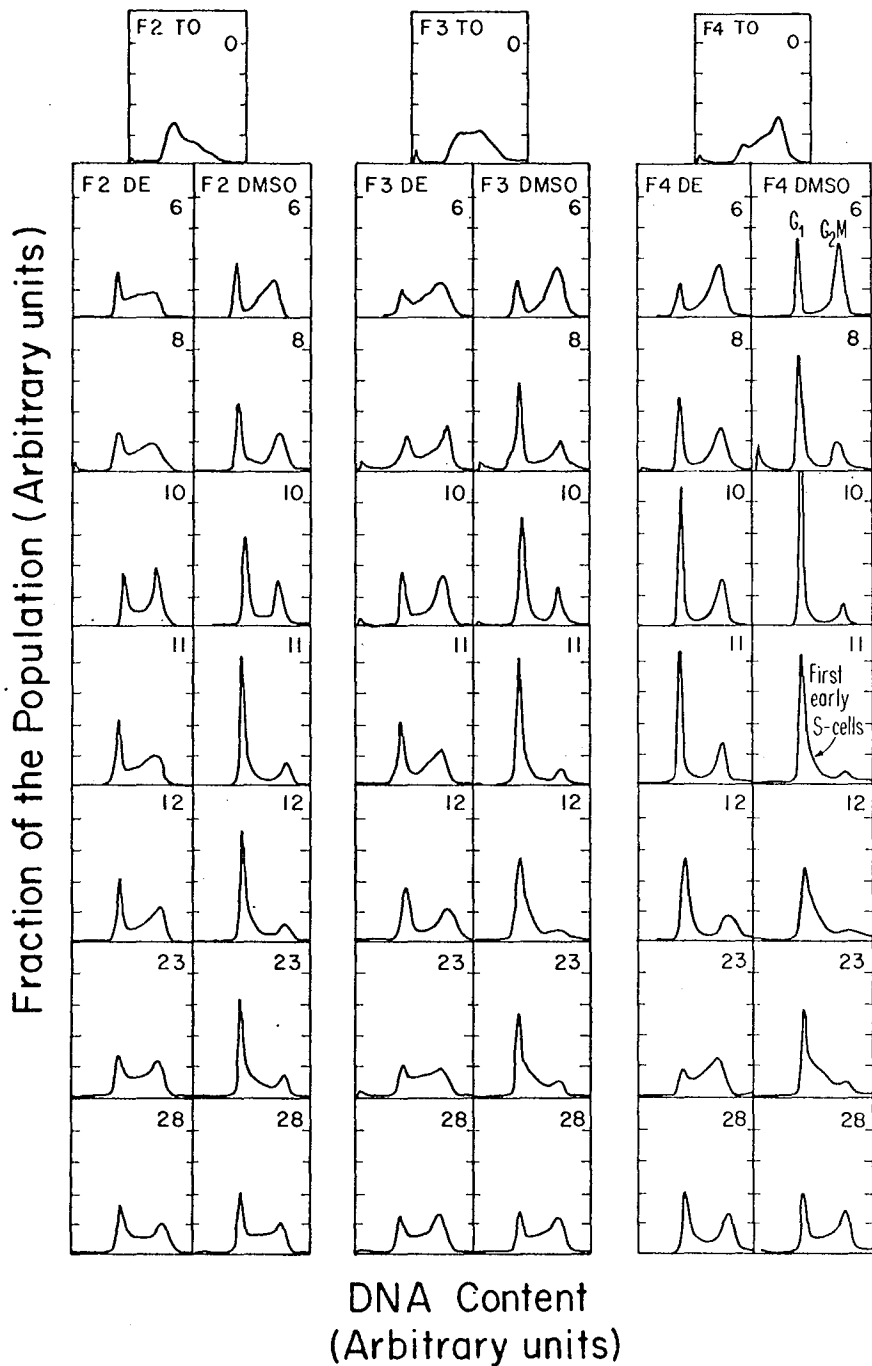
CHART 3



XBL 788-4169A



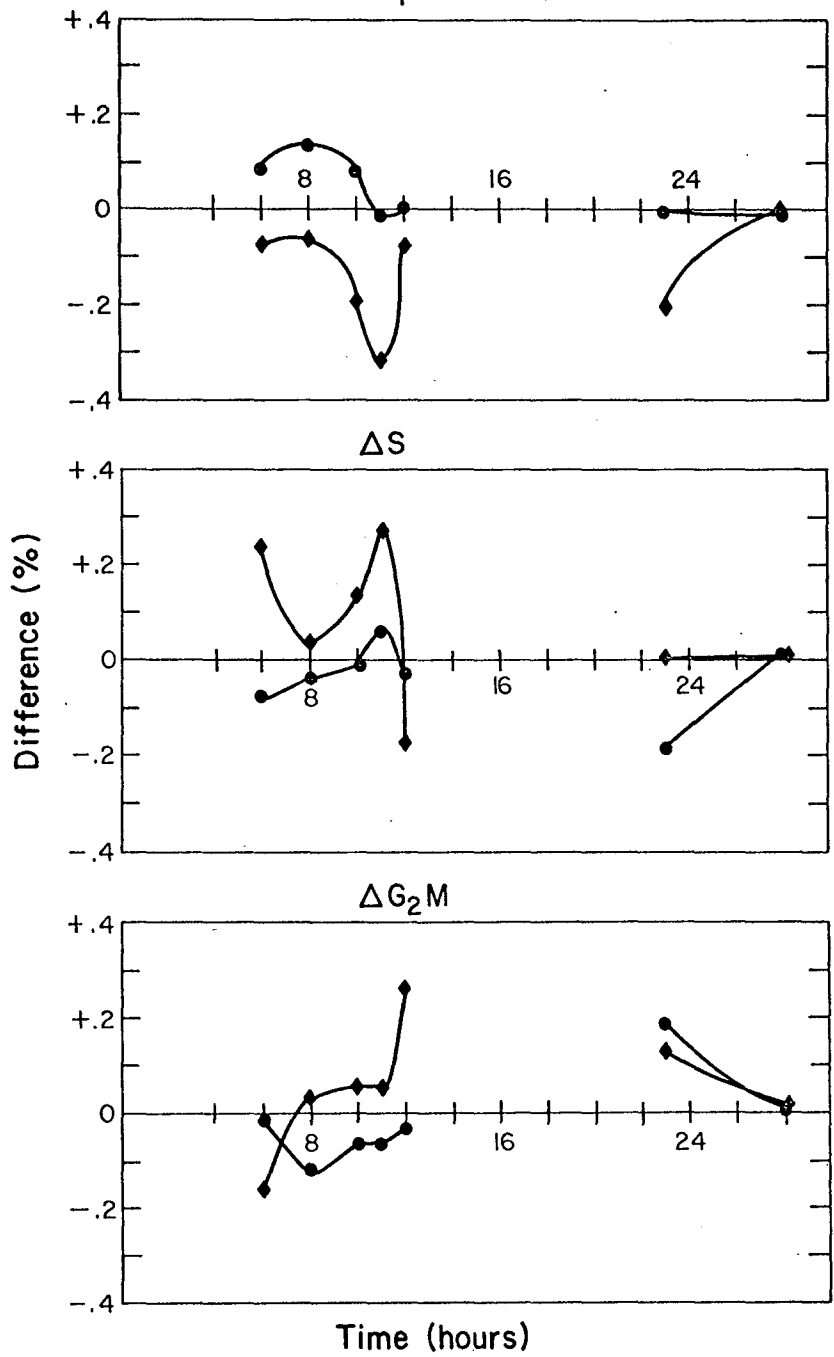
DIOL EPOXIDE (DE) vs DMSO SOLVENT, hours



XBL 788-4170A

### NET EFFECTS ON CYCLE PHASES

$\Delta G_1$  F1:• F3:♦



XBL 786-4042 A

This report was done with support from the United States Energy Research and Development Administration. Any conclusions or opinions expressed in this report represent solely those of the author(s) and not necessarily those of The Regents of the University of California, the Lawrence Berkeley Laboratory or the United States Energy Research and Development Administration.